Limited Contribution of Preferential Dissolution to Radiogenic Uranium Isotope Disequilibrium Observed in Weathered Moraines

Laifeng Li[1, 2, 4], **Laura F. Robinson**[3], **Tianyu Chen**[1], **Zhewen Xu**[1, 4], **Jun Chen**[1, 4], **Gaojun Li**[*1, 4]

1. *MOE Key Laboratory of Surficial Geochemistry, Department of Earth and Planetary Sciences,
Nanjing University, Nanjing* 210023, *China*
2. *School of Geography and Ocean Science, Nanjing University, Nanjing* 210023, *China*
3. *School of Earth Sciences, University of Bristol, Bristol BS*8 1*RJ, UK*
4. *Frontiers Science Center for Critical Earth Material Cycling, Nanjing University, Nanjing* 210023, *China*

Laifeng Li: https://orcid.org/0000-0003-3223-3397; Gaojun Li: https://orcid.org/0000-0002-2463-0774

**ABSTRACT: Radiogenic uranium isotope disequilibrium ($^{234}U/^{238}U$) has been used to trace a variety of Earth surface processes, and is usually attributed to direct recoil of ^{234}Th and preferential dissolution of radioactively damaged lattices at the mineral surface. However, the relative contribution of these two mechanisms in the natural environment remains unresolved, making it hard to use the extent of disequilibrium to quantify processes such as weathering. This study tests the contribution of preferential dissolution using well-characterized weathered moraines and river sediments from the southeastern Tibetan Plateau. Our observations show that weathering of recent moraines where the contribution from direct recoil is negligible and is not associated with depletion of ^{234}U at the mineral surface. It suggests a limited role for preferential dissolution in this setting. We attribute this lack of preferential dissolution to a near-to-equilibrium dissolution at the weathering interfaces, with little development of etch pits associated with radioactively damaged energetic sites.
KEY WORDS: preferential dissolution, uranium isotope disequilibrium, Gongga Mountain, comminution, comminution age, etch pits.**

0 INTRODUCTION

Radiogenic uranium isotope disequilibrium, expressed as the activity ratio between ^{234}U and ^{238}U ($^{234}U/^{238}U$), has shown great potential for tracing Earth surface processes (Liang and Tian, 2021; Dosseto, 2014; Chabaux et al., 2008, 2003; Bourdon et al., 2003), such as the hydrological cycle (Huckle et al., 2016; Lidman et al., 2016; Durand et al., 2005; Riotte and Chabaux, 1999), weathering rates and timescales (Dosseto et al., 2019, 2014, 2006a; Ma et al., 2019, 2012; Li L F et al., 2018; Chabaux et al., 2013; Keech et al., 2013; Pogge von Strandmann et al., 2010; Pelt et al., 2008; Maher et al., 2006, 2004; Vigier et al., 2001; Moreira-Nordemann, 1980), and marine and terrestrial sediment transport (Thollon et al., 2020; Li L et al., 2018; Li C et al., 2016, 2015; Handley et al., 2013; Granet et al., 2010; Dosseto et al., 2008, 2006b, c; DePaolo et al., 2006). The ($^{234}U/^{238}U$) of terrestrial waters and weathered sediment typically differ from that of the expected bedrock secular equilibrium ($^{234}U/^{238}U$) value of one (DePaolo et al., 2006; Bourdon et al., 2003; Dunk et

al., 2002). It is critical to understand the processes behind this disequilibrium in order to make accurate interpretations. Two main mechanisms have been invoked to explain the isotope disequilibrium: direct recoil and preferential dissolution. The direct recoil mechanism refers to ejection of ^{234}Th, the precursor of ^{234}U, associated with alpha-decay of the ^{238}U nuclei near the mineral surface (Li L et al., 2017; DePaolo et al., 2012, 2006; Kigoshi, 1971). Preferential dissolution refers to dissolution of ^{234}U from sites that have been radioactively damaged by alpha-decay of ^{238}U (Andersen et al., 2009; Bourdon et al., 2009; Fleischer, 1982, 1980). This mechanism relies on alpha-recoil tracks exposed to the mineral surface connecting the ^{234}U sites with the surrounding solution (Hussain and Lal, 1986; Fleischer and Raabe, 1978), facilitating the release of ^{234}U.

Despite its importance to interpret the uranium isotope disequilibrium, evidence of preferential dissolution remains elusive. In the experiments of Fleischer (1982, 1980), the loss of radioactively implanted ^{235}U in mineral surfaces after leaching could have been associated with true dissolution of the very surface layer of the mineral rather than preferential dissolution from alpha-recoil tracks. Testing for preferential dissolution by annealing experiments failed to give consistent and conclusive results among different minerals (Fleischer, 1982). Leaching experiments on natural mineral of monazite showed contrasting results between specimens from different places

(Eyal and Olander, 1990). Radiogenic uranium isotope disequilibrium was observed during initial leaching of the natural monazite and congruent dissolution of ^{234}U and ^{238}U was observed for the annealed monazite, which is consistent with the prediction of preferential dissolution. However, disequilibrium was not observed in a second monazite from a different location under the same dissolution condition either for the annealed or unheated specimens (Eyal and Olander, 1990). Andersen et al. (2009) investigated natural granites and showed enrichment of ^{234}U in the solute during an initial leaching stage. However, the enrichment of ^{234}U may also result from heterogeneity of uranium among different minerals or within a mineral (Rihs et al., 2020; Bosia et al., 2018; Dosseto et al., 2014; Robinson et al., 2006). Recoil ejection of ^{234}Th from minerals with high uranium concentration would result in enrichment of ^{234}U relative to ^{238}U in neighboring minerals with low uranium concentration (Robinson et al., 2006). Preferential dissolution of the minerals with low uranium concentration may then have contributed to the radiogenic uranium isotope disequilibrium in these leaching experiments (Andersen et al., 2009; Bourdon et al., 2009; Bonotto et al., 2001; Bonotto and Andrews, 1993; Hussain and Lal, 1986; Zielinski et al., 1982).

This study assesses the contribution of preferential dissolution to uranium isotope disequilibrium using well-characterized glacial moraines. The rationale is that depletion of ^{234}U at the mineral surface would not be prominent for young moraines of < ~20 ka without preferential dissolution due to the limited time for accumulating the direct recoiling effect.

1   SAMPLES AND METHODS

1.1   Sample Collection

Moraines and sediments from the modern glacial outlet were collected from the Gongga Mountain area (Fig. 1), where the bedrock mainly consists of granite. Several factors make the glacial moraines on the southeastern margin of Tibetan Plateau unusually well-suited materials for such an investigation. The glacier fronts and associated moraines in this region extend into the valleys of relatively low altitude with temperate climate benefiting from high snow accumulation rates and high relief (Li Z X et al., 2010; Liu Q et al., 2010; Liu Q and Liu S Y, 2009; Su et al., 1996). The high temperature associated with the subtropical low altitude setting and the high precipitation associated with Indian monsoon enable post-glacial weathering alteration of the moraines to different degrees (Zhou et al., 2016; He and Tang, 2008). Prior research on the glacial dynamics and paleoclimate changes have resulted in extensive investigation on the age and distribution of moraines (Wang et al., 2013; Owen et al., 2005), providing important chronological constraints for this study.

Field observations based on the content of clay and accumulation of organic carbon show that the surface layer (0−20 cm) of the moraine in Gongga Mountain area generally experiences a higher degree of weathering and pedogenesis compared to its deeper counterpart (> 20 cm) and the recently produced moraines. In total, ten samples of topsoil (0−20 cm) developed on the moraines with known age from 0.34 to 149.85 ka were collected (Fig. 1, Table 1). Three samples of river sediments were collected at the leading edge of the glacier outlet to
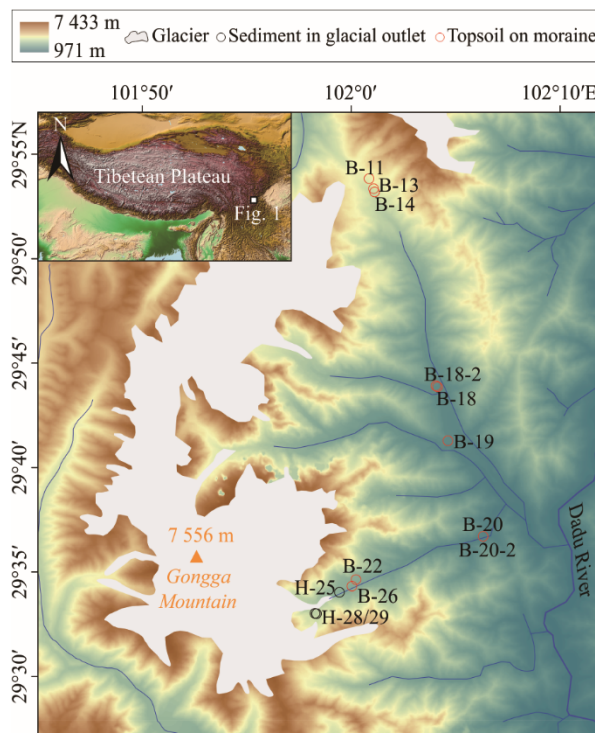
Figure 1. Maps show the sampling sites around the Gongga Mountain. Inset map shows the location of Gongga Mountain on the southeastern margin of Tibetan Plateau.

represent the freshly deposited glacial sediments because distribution of previously weathered moraine in the upper stream is rather limited (Fig. 1, Table 1). It should be noted that the relative correlation of weathering intensities among moraines with different ages is constant even if fresher glacial sediments are collected given that the glacial sediments is only regarded as a reference when calculating the weathering intensities.

In addition, river sediments on terraces with age > 1 Ma were collected in other regions worldwide to investigate the fraction of ^{234}Th that can be ejected to the surroundings along with the decay of ^{238}U and thus the fraction of ^{234}U sites that are connected to the mineral surface by recoiling tracks. Two samples were collected from the terraces along the upper reaches of Orange River in the Kingdom of Lesotho and six samples were collected from the terraces of upper reaches of Yangtze River near Dali, Yunnan Province, China (Table 2). The terraces of Orange River in Lesotho is more than 10 m higher than the present-day river channel, which predict an age of > 1 Ma considering a low regional denudation rate of ~8 mm/ka (Brown et al., 2002; Fleming et al., 1999). The terraces in Dali have been dated by Su et al. (2019) and those with age older than 1 Ma were investigated in this study.

1.2   Analytical Methods

Major element compositions of the moraine and the sediments at the leading edge of the glacier outlet were analyzed to reflect weathering intensity. The < 50 μm size fraction of the samples, which was separated by metal sieves, is used to reduce the effect of sediment sorting. The < 50 μm size fraction has higher concentration of clay than bulk sediment and is

Table 1 The uranium isotope ratio and chemical weathering proxies of topsoil developed on moraine
as well as river sediments in the present-day glacial outlet.

Name	Latitude (ºN)	Longitude (ºE)	Type	Moraine age (ka)	$(^{234}U/^{238}U)$	2SE[a]	CIA[b]	[Ca/Al] (mol/mol)	CDF_{Ca}[b]	Reference for the moraine age
GZ19B-26	29.571 6	102.000 0	Topsoil	0.34	1.003	0.001	36.4	0.58	0.33	Owen et al. (2005)
GZ19B-22	29.576 9	102.003 2	Topsoil	0.755	0.997	0.001	40.2	0.41	0.53	Owen et al. (2005)
GZ19B-19	29.687 6	102.076 6	Topsoil	4.645	1.007	0.001	62.4	0.06	0.93	Owen et al. (2005)
GZ19B-20	29.611 5	102.104 7	Topsoil	7.98	1.006	0.001	49.6	0.28	0.68	Owen et al. (2005)
GZ19B-20-2	29.611 5	102.104 7	Topsoil	7.98	1.004	0.001	55.2	0.21	0.75	Owen et al. (2005)
Average					1.003					
2SE					0.004					
GZ19B-18	29.731 4	102.067 5	Topsoil	53.6	1.002	0.001	53.0	0.09	0.90	Wang et al. (2013)
GZ19B-18-2	29.731 4	102.067 5	Topsoil	53.6	0.986	0.001	58.2	0.14	0.83	Wang et al. (2013)
GZ19B-11	29.896 6	102.013 6	Topsoil	94.5	0.988	0.001	67.8	0.07	0.92	Wang et al. (2013)
GZ19B-14	29.886 2	102.018 0	Topsoil	137.7	0.998	0.001	72.8	0.05	0.94	Wang et al. (2013)
GZ19B-13	29.888 5	102.017 6	Topsoil	149.85	0.991	0.001	54.9	0.15	0.83	Wang et al. (2013)
Average					0.993					
2SE					0.006					
GZ19H-25	29.566 9	101.990 1	Sediment	/[c]	1.004	0.001	29.2	0.92	/	/
GZ19H-28	29.549 7	101.971 7	Sediment	/	1.007	0.001	29.1	0.99	/	/
GZ19H-29	29.550 1	101.970 5	Sediment	/	1.014	0.001	32.1	0.68	/	/
Average of river sediments					1.008		30.1	0.86		
2SE					0.006		2.0	0.19		

[a]. 2SE is the analytical error given by MC-ICP-MS. The external error of the whole analytical procedure is ± 0.004; [b]. CIA is the chemical index of alteration; CDF_{Ca} is chemical depletion fraction of Ca relative to Al; [c]. "/" means not applicable

Table 2 The uranium isotope ratios of sediments on river terraces

Sample No.[a]	Latitude (N)	Longitude (E)	Age (Ma)	$(^{234}U/^{238}U)$	2SE[b]	Reference for the age
LST44	-29.596 0	28.713 4	> 1	0.896	0.001	This study
LST62	-29.019 8	28.548 5	> 1	0.897	0.001	This study
DL19S-14-2	26.226 2	100.507 8	1.07	0.900	0.001	Su et al. (2019)
DL19S-14	26.227 0	100.507 4	1.07	0.901	0.001	Su et al. (2019)
DL19S-12-2	26.234 0	100.505 1	1.5	0.903	0.001	Su et al. (2019)
DL19S-12	26.234 0	100.505 1	1.5	0.902	0.001	Su et al. (2019)
DL19S-13	26.232 8	100.505 6	1.5	0.916	0.001	Su et al. (2019)
DL19S-13-2	26.232 8	100.505 6	1.5	0.909	0.001	Su et al. (2019)

[a]. Sample labeled by LST is from upper reaches of Orange River in Lesotho, and samples labeled by DL is from upper reaches of Yangtze River near Dali, China; [b]. 2SE is the analytical error given by MC-ICP-MS. The external error of the whole analytical procedure is ± 0.004.

therefore more likely to show the difference in weathering intensities. The sieved fraction was then digested in clean lab in 4 mL 1 : 1 mixture of HNO_3 and HF solution in tightly sealed Teflon vials at 120 °C for more than 36 h. The concentrations of major elements are measured by a quadruple ICP-MS with an external error better than 5%.

The 20−25 μm fine silt fraction of moraines, sediments in glacial outlet, and terrace sediments is chosen to investigate the uranium isotope disequilibrium because the effect of recoil ejection and assumed preferential dissolution on $(^{234}U/^{238}U)$ is prominent only in the fine particles (DePaolo et al., 2006). The method of Li L et al. (2017) is followed to separate the 20−25 μm fine detrital silt fractions, remove the authigenic phases (carbonate, Fe-Mn hydroxide coating and organic matter), and

digest the extracted fine detrital silt fractions. The uranium in the digested solutions was separated using UTEVA resin, following the method in Wang and You (2013b). The $(^{234}U/^{238}U)$ ratios were measured by a MC-ICP-MS (Neptune Plus) in MOE Key Laboratory of Surficial Geochemistry of Nanjing University, China according to the same method of Li L et al. (2017). The U.S. Geological Survey BCR-2 standard material is measured to check the accuracy of measurement, giving an equilibrium $(^{234}U/^{238}U)$ ratio of 1.000 ± 0.001 (mean ± 2 × standard error), which is consistent with the recommended values (e.g., Bragagni et al., 2014). Two loess samples with age > 1 Ma were also measured to monitor the accuracy of whole chemical procedures, which gives $(^{234}U/^{238}U)$ ratios of 0.915 ± 0.001 and 0.914 ± 0.001 (mean ± 2 × standard error) of the 20−

25 μm fine detrital silt fractions, respectively. Those values are consistent with the long-term measurement value of 0.912 within error (Li et al., 2017) considering an external error of 0.004 (2 × standard deviation) of the whole analytical procedure.

2 RESULTS

The weathering intensity of topsoils developed on moraines can be characterized by the chemical depletion fraction of mobile element (CDF) and chemical index of alteration (CIA). The chemical depletion fraction of Ca (CDF_{Ca}) is calculated by depletion of highly mobile element of Ca related to the immobile element of Al.

$$CDF_{Ca} = 1 - [\,Ca/Al\,]_{moraine} / [\,Ca/Al\,]_{outlet} \qquad (1)$$

where the subscripts moraine and outlet represent topsoil developed on moraine and sediment at the leading edge of the present-day glacial outlet, respectively. The calculation of chemical index of alteration (CIA) follows the equation of Nesbitt and Young (1982).

$$CIA = [\,Al_2O_3 / (\,Al_2O_3 + CaO^* + Na_2O + K_2O\,)\,] \times 100 \qquad (2)$$

where all oxides represent molar content of those oxides and CaO* is the CaO molar content of silicate. The carbonate content in our samples is negligible so that correction of carbonate for CaO* does not apply.

The CDF_{Ca} and CIA of the topsoil developed on moraines

in Gongga Mountain area show a wide range from 0.33 to 0.94, and from 36.4 to 72.8, respectively (Table 1). Both CDF_{Ca} and CIA indicate a positive correlation between weathering intensity of the topsoil and the age of the moraine with slower increase of weathering intensity for the aged deposits (Fig. 2).

The ($^{234}U/^{238}U$) values of 20−25 μm fine detrital silt fraction of all topsoils have a narrow range from 0.986 to 1.007. Topsoils developed on young moraine (< 20 ka) have an average ($^{234}U/^{238}U$) value of 1.003±0.004 (mean ±2SE) that are slightly higher than those developed on aged moraines (> 20 ka; 0.993±0.006). The average ($^{234}U/^{238}U$) value of topsoil developed on young moraine is close to that of the sediments in the present-day glacial outlet (1.008±0.006). No correlation can be observed between ($^{234}U/^{238}U$) ratios and weathering intensities reflected by CDF_{Ca} and CIA (Fig. 3).

The ($^{234}U/^{238}U$) ratios of two terrace sediments in Lesotho show consistent values of 0.896 and 0.897, respectively (Table 2, Fig. 4). The terrace sediments in Dali give a narrow range of ($^{234}U/^{238}U$) value from 0.900 to 0.916 (Table 2, Fig. 4).

3 DISCUSSION

3.1 Preferential Dissolution Tested by the Moraines

CDF and CIA are widely used to reflect the weathering intensities (e.g., Lü et al., 2016; Riebe et al., 2001). The values of CIA and CDF_{Ca} (Table 1, Fig. 2) confirm the field observa-
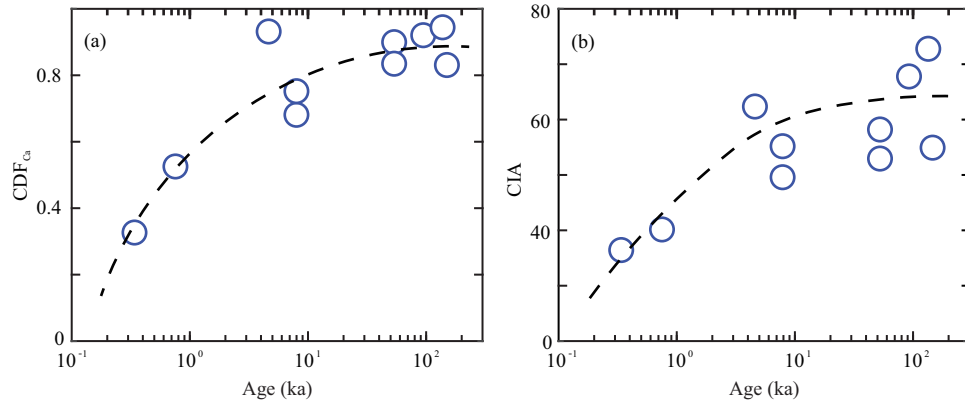
Figure 2. Correlating the (a) chemical depletion fraction of Ca (CDF_{Ca}) and (b) chemical index of alteration (CIA) of the topsoils developed on the moraine to the age of moraine. Black dashed lines show the empirically determined trend.
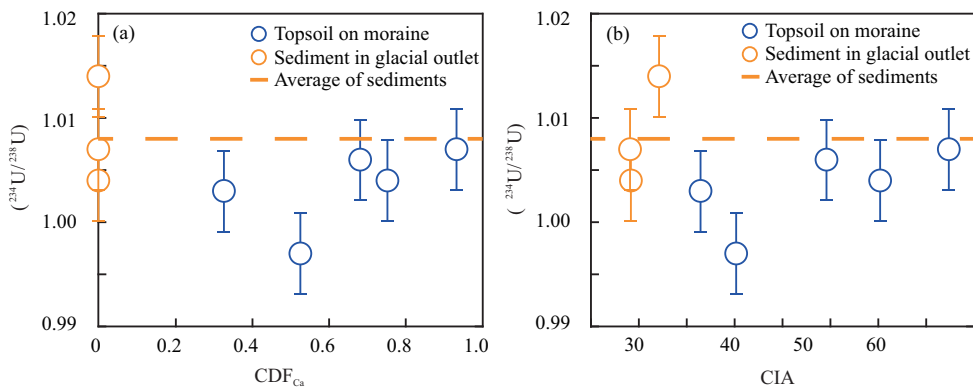
Figure 3. The ($^{234}U/^{238}U$) ratios of 20−25 μm fine silt fraction of the topsoil developed on young moraines (< 20 ka) and the river sediments in glacial outlet plotting against the chemical weathering indices. The CDF_{Ca} of river sediments is zero because the parent material for CDF_{Ca} calculation is based on the sediments in the glacial outlet. Dashed lines indicate the average of river sediments that represents the initial value.
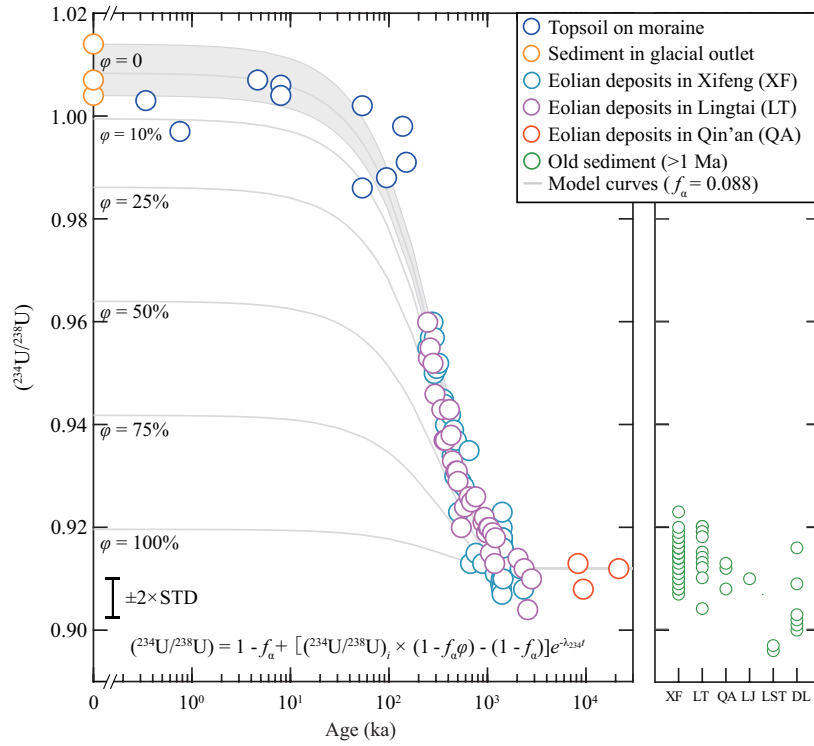
Figure 4. Model calculation show the combined effects of preferential dissolution and recoil ejection on uranium isotope disequilibrium. The data of eolian deposits is from Li L et al. (2017). The grey band shows the model result under variable $(^{234}\mathrm{U}/^{238}\mathrm{U})_i$ ratios (based on the $(^{234}\mathrm{U}/^{238}\mathrm{U})$ ratios of sediments in glacial outlet) and constant fraction of preferential dissolution ($\varphi = 0$). The comminution age of eolian sediments is calculated from deposition age plus the transportation time constrained by Li L et al. (2017). Green circles represent the $(^{234}\mathrm{U}/^{238}\mathrm{U})$ ratios of sediments with age > 1 Ma. The labels of XF, LT, and QA represent the eolian deposits in Xifeng, Lingtai and Qin'an sites from Li L et al. (2017), LJ represents the lacustrine sediment at Laja site from Li L et al. (2020); LST and DL represents the terrace sediments of upper reaches of Orange River in Lesotho and upper reaches of Yangtze River near Dali, China.

tion that the surface layer of the moraine has been weathered to different degrees. The highest $\mathrm{CDF_{Ca}}$ of 0.94 indicates a nearly complete dissolution of the Ca-containing minerals. The positive correlation between weathering indices and moraine age is consistent with the expected influence of surface exposure time on the accumulated weathering depletion (Fig. 2). The correlation between chemical depletion and moraine age also indicates attenuation of weathering rate with time, which is consistent with the observations from soil chronosequences (White et al., 2009, 2008, 1996; Taylor and Blum, 1995) and the results of laboratory leaching experiments (White and Brantley, 2003).

The nearly identical $(^{234}\mathrm{U}/^{238}\mathrm{U})$ values of detrital young moraines compared to the sediment in the present-day glacial outlet (Fig. 3) argues for a limited contribution of preferential dissolution to the uranium isotope disequilibrium. This is because cumulative depletion of $^{234}\mathrm{U}$ caused by recoil ejection is negligible for these young (< 20 ka) moraines (Fig. 4). Thus, any preferential dissolution of $^{234}\mathrm{U}$ would decrease the $(^{234}\mathrm{U}/^{238}\mathrm{U})$ value of moraines. The influence of preferential dissolution may also generate a correlation between $(^{234}\mathrm{U}/^{238}\mathrm{U})$ and weathering intensity, which is not supported by the observations (Fig. 3). The slightly lower $(^{234}\mathrm{U}/^{238}\mathrm{U})$ value of aged moraines (> 20 ka) can be explained by the effect of direct recoiling (Fig. 4).

It is possible that preferential dissolution of $^{234}\mathrm{U}$ in mineral surface is occurring, but the specific surface area of the analyzed fine silt particles is so small that the effects of preferential

dissolution cannot be detected in the $(^{234}\mathrm{U}/^{238}\mathrm{U})$ value. Here a model is developed to investigate such a possibility. Without the effect of preferential dissolution, the $(^{234}\mathrm{U}/^{238}\mathrm{U})$ ratios of glacial sediments would decrease with time since its comminution owing to direct recoil ejection of $^{234}\mathrm{Th}$ (DePaolo et al., 2012, 2006).

$$\left(^{234}\mathrm{U}\big/^{238}\mathrm{U}\right) = \left(1 - f_\alpha\right) + \left[\left(^{234}\mathrm{U}\big/^{238}\mathrm{U}\right)_0 - \left(1 - f_\alpha\right)\right]e^{-\lambda_{234}t} \quad (3)$$

where f_α is the fraction of $^{234}\mathrm{Th}$ that are rejected to the surroundings along the decay of $^{238}\mathrm{U}$, $(^{234}\mathrm{U}/^{238}\mathrm{U})_0$ represents the original activity ratio of the sediment, λ_{234} is the decay constant of $^{234}\mathrm{U}$, and t is the age of moraines since comminution. The value of f_α depends on specific area of the particle, with smaller grain size and higher roughness the higher f_α. Measuring the f_α directly is challenging owing to the fractal feature of particle surface (DePaolo et al., 2012, 2006; Lee et al., 2010; Bourdon et al., 2009; Maher et al., 2006).

Preferential dissolution is assumed to take place quickly and complete within a short timescale since the comminution of particle considering the much higher dissolution rate of uncrystallized glass (similar to the damaged sites) compared to crystals of similar chemical composition (Brantley and Olsen, 2014), therefore it mainly affects the initial $(^{234}\mathrm{U}/^{238}\mathrm{U})$ ratio. We express the effect of preferential dissolution through the $(^{234}\mathrm{U}/^{238}\mathrm{U})_0$ ratio.

$$\left(^{234}\mathrm{U}\big/^{238}\mathrm{U}\right)_0 = \left(^{234}\mathrm{U}\big/^{238}\mathrm{U}\right)_i \times \left(1 - f_p\varphi\right) \quad (4)$$

where the $(^{234}U/^{238}U)_i$ is the initial $(^{234}U/^{238}U)$ value of freshly produced sediment before weathering, f_p is fraction of total ^{234}U with damaged crystal tracks that connect to minerals surface, φ is the fraction of surface-connected ^{234}U that is preferentially dissolved. The value of $(^{234}U/^{238}U)_i$ is generally to be 1 for the freshly comminuted rocks under secular equilibrium but would be slightly higher due to effect that has not been fully understood (DePaolo et al., 2012). One of the possible explanation for the enrichment of ^{234}U may result from heterogeneity of uranium among different minerals or within a mineral (Rihs et al., 2020; Bosia et al., 2018; Dosseto et al., 2014; Robinson et al., 2006). A simple geometric consideration shows that the value of f_p is same as f_a (Hussain and Lal, 1986), i.e., within the very surface layer of mineral less than a recoiling distance beneath mineral surface, 25% of ^{234}U sites is connected to mineral surface by recoiling tracks and 25% of ^{234}Th produced by ^{238}U decay would be ejected. Combining Eqs. (3) and (4) give

$$\left(^{234}U \middle/ {}^{238}U\right) = \left(1 - f_a\right) +$$
$$\left[\left(^{234}U \middle/ {}^{238}U\right)_i \times \left(1 - f_a \varphi\right) - \left(1 - f_a\right)\right] e^{-\lambda_{234} t} \qquad (5)$$

Eq. (5) makes it possible to evaluate the effect of preferential dissolution on $(^{234}U/^{238}U)$ ratios, which largely depends on the value of f_a. A small value of f_a would result a small value of $f_a\varphi$ so that preferential dissolution will not influence the $(^{234}U/^{238}U)$ ratio of sediment. However, we think this scenario is unlikely because large value of f_a can be inferred from old sediments with age > 1 Ma where the term $e^{-\lambda_{234} t}$ in Eq. (5) approaches to zero, and Eq. (5) can be simplified to

$$\left(^{234}U \middle/ {}^{238}U\right)_{>1Ma} \approx 1 - f_a \qquad (6)$$

a compilation of published $(^{234}U/^{238}U)$ ratios of old (> 1 Ma) sediments (Li L et al., 2020, 2017) and new measurements of terrace sediments with age of > 1 Ma in this study gives a narrow range of f_a value from 0.088 to 0.106 (Fig. 4, Table 2). The variation of f_a values could result from changes in surface roughness due to different types of sediments (DePaolo et al., 2006). The higher f_a values of terrace sediments from Lesotho may be caused by the porous character of basaltic sediment. A lower f_a values of 0.088 for the loess deposits on the Chinese Loess Plateau may result from smooth particle surface associated with the glacial grinding that produces the loess particles (Sun, 2002; Smalley, 1995). We think that the f_a values of moraines could be similar to that of loess due to the same glacial grinding that produces the particles.

Comparing the model prediction of Eq. (5) with $(^{234}U/^{238}U)$ ratio of glacial sediments results in maximum value of φ of < 10% using a minimum estimated f_a value of 0.088 and a value of $(^{234}U/^{238}U)_i$ inferred from the river sediments in the present-day glacial outlet (Fig. 4). Higher values of φ would predict a much lower $(^{234}U/^{238}U)$ ratio than the young sediments (Fig. 4). A complete preferential dissolution of ^{234}U nuclei that connect to mineral surface by recoiling track, i.e., $\varphi = 100\%$, would generate $(^{234}U/^{238}U)$ ratio of 0.920 (Fig. 4). The maximum value of φ implies that less than 10% of surface-connecting ^{234}U sites are preferentially dissolved. Thus, preferential dissolution of ^{234}U appears to have a limited contribution to the uranium isotope disequilibrium.

3.2 Limited Preferential Dissolution Inferred from Other Evidences

The limited contribution of preferential dissolution to the uranium isotope disequilibrium is also supported by the application of uranium isotope comminution age (Li L et al., 2020, 2018, 2017; DePaolo et al., 2006). The method of 'comminution age' relies on direct recoil ejection of ^{234}Th from mineral surfaces so that deficiency of ^{234}U in the mineral surface, relative to ^{238}U, increases with time since comminution (DePaolo et al., 2012, 2006). Theoretically, preferential dissolution would also induce depletion of ^{234}U in the particle surface. A complete removal of the ^{234}U sites connected to the mineral surface along recoil tracks would pre-equilibrate the system so that the subsequent recoil effect would not decrease the $(^{234}U/^{238}U)$ ratio. However, this inference is not supported by the strong correlation between $(^{234}U/^{238}U)$ of fine silt and deposition age observed from the Chinese loess deposits (Li L et al., 2017), indicating there is not a complete dissolution of the alpha-recoil tracks that are connected to mineral surface.

The $(^{234}U/^{238}U)$ of river water also indicates limited contribution of preferential dissolution to the uranium isotope disequilibrium. A simple calculation demonstrates that preferential dissolution is only likely to cause measurable disequilibrium if the weathering intensity is so low that a thickness equivalent to only a few layers of recoiling distance (~20.8 nm, Nasdala et al., 2001) beneath the mineral surface is dissolved away (Hussain and Lal, 1986). With enhanced weathering, the weathering interface would rapidly dissolve away the ^{234}U-depleted layer although preferential ^{234}U release may still operate at the dissolution front. For example, weathering of more than 10 layers of recoiling distance would result in a $(^{234}U/^{238}U)$ of less than 1.025 (Hussain and Lal, 1986) considering that 25% of ^{234}U in the mineral surface within a recoiling distance could be preferentially dissolved (Kigoshi, 1971), much lower than most river waters (Li L F et al., 2018). Thus, a lower $(^{234}U/^{238}U)$ value (close to the secular equilibrium value) in the dissolved load is expected in regions with higher weathering intensity. However, a global compilation indicates a higher $(^{234}U/^{238}U)$ of river water in catchment with lower denudation rate, and thus higher chemical weathering intensity (Li L F et al., 2018). It suggests that river water mainly gain their high $(^{234}U/^{238}U)$ by direct recoiling. A longer regolith residence time associated with lower denudation rate results in higher accumulation of direct recoil ^{234}U (Li L F et al., 2018). Interpreting uranium isotope disequilibrium of river waters as being caused by preferential leaching requires very low chemical weathering intensity, a condition that is likely applicable only to the terrains such as New Zealand and Taiwan Island where physical erosion dominates (Li L F et al., 2018; Robinson et al., 2004).

3.3 Mechanisms for Limited Preferential Dissolution

The limited contribution of preferential dissolution to the uranium isotope disequilibrium may result from a transport-controlled dissolution of the radioactively damaged sites. Preferential dissolution would generate an etch pit that increases the distance of diffusive transportation between the dissolving

site of the alpha-recoil track and the particle surface, which may result in higher saturation state of fluid around the dissolving site. The high saturation state of fluid at the weathering interface may also be caused by the development of surface precipitates as observed both in field and laboratory (Parruzot et al., 2015; Ruiz-Agudo et al., 2012; Daval et al., 2011). Meanwhile, our result may mainly reflect the weathering resistant minerals such as zircon, whose saturation state may be different from the dominant silicate minerals. It has been shown that the dissolution rate decreases dramatically with increasing saturation at near-to-equilibrium state (Brantley and Olsen, 2014; Nagy and Lasaga, 1992). Thus, the etch pit associated with alpha-recoil track may stop advancing once the dissolution rate at the front of the etch pit decreases to the level of surface retreat in response to the increasing saturation level. It is possible that only a few percent of the recoiling distance are required to increase the saturation to a near-to-equilibrium level so that only the ^{234}U associated with very shallow alpha-recoil track can be preferentially released.

The preferential dissolution of the alpha-recoil track may also be inhibited by the surface energy associated with the development of etch pit. It has been shown that, in case of high saturation state of the solution, the energy released by dissolution cannot compensate for the associated surface energy if the etch pit is below a critical size (Brantley et al., 1986; Lasaga and Blum, 1986). The critical size for spontaneous growth of etch pit depends on the saturation state of the solution and thus the chemical affinity associated with dissolution. Thus, it is possible that the saturation state of the solution is high enough so that etch pit would not grow spontaneously along the alpha-recoil track.

The control of saturation state on preferential dissolution suggests that the limited contribution of preferential dissolution to the uranium isotope disequilibrium may apply only to the cases where the saturation states of uranium-containing minerals are high with respect to solution. However, determination of the *in-situ* saturation state of the minerals in natural environment is rather difficult because composition of the solution at mineral surfaces may be very different from the solution in connected pore water that may be reflected by seepage and river water. Nevertheless, we think regions with a dry climate and thus concentrated soil solution would likely have mineral surfaces that are subjected to limited preferential dissolution. Thus, uranium isotope comminution age can be successfully applied to the eolian loess deposits in arid and semi-arid regions (Li L et al., 2017). We also predict a limited contribution of preferential dissolution to the uranium isotope disequilibrium at deep sites of a regolith where the saturation is generally high (Riebe et al., 2017). However, we cannot exclude the possibility that in regions with extremely high precipitation, such as New Zealand and Taiwan Island (Wang and You, 2013a; Robinson et al., 2004), preferential weathering may operate considering the high (^{234}U/^{238}U) ratios of river water that are unlikely accumulated from direct recoil ejection due to the short residence time of regolith under rapid erosion and the increasing riverine (^{234}U/^{238}U) with increasing denudation rate (Robinson et al., 2004).

4 CONCLUSION

This study measured the ^{234}U/^{238}U ratios of silt fraction of glacial moraines with known age from the southeastern margin (Gongga Mountain area) of the Tibetan Plateau. The results show that the ^{234}U/^{238}U ratios of young (< 20 ka) silt glacial sediments remain the initial values in spite of various weathering intensities, indicating limited influence of preferential dissolution on uranium isotope disequilibrium. Inhibition of etch pit growth and diffusion-limited dissolution of the deeply seated damaged mineral lattices caused by high solute concentration may explain the limited influence of preferential dissolution on uranium isotope disequilibrium. The limited contribution of preferential dissolution to the ^{234}U depletion of particle surface confirm the robustness of the application of uranium comminution age method. Fluid residence time, and thus accumulation of recoil ejected ^{234}U, may be a key factor to control the uranium isotope disequilibrium of natural water in most cases.

REFERENCES CITED

Andersen, M. B., Erel, Y., Bourdon, B., 2009. Experimental Evidence for ^{234}U-^{238}U Fractionation during Granite Weathering with Implications for ^{234}U/^{238}U in Natural Waters. *Geochimica et Cosmochimica Acta*, 73 (14): 4124−4141. https://doi.org/10.1016/j.gca.2009.04.020

Bonotto, D. M., Andrews, J. N., 1993. The Mechanism of ^{234}U/^{238}U Activity Ratio Enhancement in Karstic Limestone Groundwater. *Chemical Geology*, 103(1/2/3/4): 193−206. https://doi.org/10.1016/0009-2541(93)90301-x

Bonotto, D. M., Andrews, J. N., Darbyshire, D. P. F., 2001. A Laboratory Study of the Transfer of ^{234}U and ^{238}U during Water-Rock Interactions in the Carnmenellis Granite (Cornwall, England) and Implications for the Interpretation of Field Data. *Applied Radiation and Isotopes*, 54(6): 977−994. https://doi.org/10.1016/s0969-8043(00)00338-9

Bosia, C., Chabaux, F., Pelt, E., et al., 2018. U-Series Disequilibria in Minerals from Gandak River Sediments (Himalaya). *Chemical Geology*, 477: 22−34. https://doi.org/10.1016/j.chemgeo.2017.11.026

Bourdon, B., Bureau, S., Andersen, M. B., et al., 2009. Weathering Rates from Top to Bottom in a Carbonate Environment. *Chemical Geology*, 258(3/4): 275−287. https://doi.org/10.1016/j.chemgeo.2008.10.026

Bourdon, B., Turner, S., Henderson, G. M., et al., 2003. Introduction to U-Series Geochemistry. *Reviews in Mineralogy & Geochemistry*, 52(1): 1−21. https://doi.org/10.2113/0520001

Bragagni, A., Avanzinelli, R., Freymuth, H., et al., 2014. Recycling of Crystal Mush-Derived Melts and Short Magma Residence Times Revealed by U-Series Disequilibria at Stromboli Volcano. *Earth and Planetary Science Letters*, 404: 206−219. https://doi. org/10.1016/j.

epsl.2014.07.028

Brantley, S. L., Crane, S. R., Crerar, D. A., et al., 1986. Dissolution at Dislocation Etch Pits in Quartz. *Geochimica et Cosmochimica Acta*, 50 (10): 2349−2361. https://doi.org/10.1016/0016-7037(86)90087-6

Brantley, S. L., Olsen, A. A., 2014. Reaction Kinetics of Primary Rock-Forming Minerals under Ambient Conditions. *Treatise on Geochemistry* (*Second Edition*), 7: 69−113. https://doi. org/10.1016/b978-0-08-095975-7.00503-9

Brown, R. W., Summerfield, M. A., Gleadow, A. J. W., 2002. Denudational History along a Transect across the Drakensberg Escarpment of Southern Africa Derived from Apatite Fission Track Thermochronology. *Journal of Geophysical Research*: *Solid Earth*, 107 (B12): ETG10-1−ETG10-18. https://doi.org/10.1029/2001jb000745

Chabaux, F., Blaes, E., Stille, P., et al., 2013. Regolith Formation Rate from U-Series Nuclides: Implications from the Study of a Spheroidal Weathering Profile in the Rio Icacos Watershed (Puerto Rico). *Geochimica et Cosmochimica Acta*, 100: 73−95. https://doi. org/10.1016/j.gca.2012.09.037

Chabaux, F., Bourdon, B., Riotte, J., 2008. Chapter 3 U-Series Geochemistry in Weathering Profiles, River Waters and Lakes. *Radioactivity in the Environment*, 13: 49−104. https://doi.org/10.1016/s1569-4860(07)00003-4

Chabaux, F., Riotte, J., Dequincey, O., 2003. U-Th-Ra Fractionation during Weathering and River Transport. In: Bourdon, B., Henderson, G. M., Lundstrom, C. C., et al., eds., Uranium-Series Geochemistry. De Gruyter, Boston. 533−576. https://doi.org/10.1515/9781501509308-018

Daval, D., Sissmann, O., Menguy, N., et al., 2011. Influence of Amorphous Silica Layer Formation on the Dissolution Rate of Olivine at 90 ºC and Elevated pCO$_2$. *Chemical Geology*, 284(1/2): 193−209. https://doi.org/10.1016/j.chemgeo.2011.02.021

DePaolo, D. J., Lee, V. E., Christensen, J. N., et al., 2012. Uranium Comminution Ages: Sediment Transport and Deposition Time Scales. *Comptes Rendus Geoscience*, 344(11/12): 678687. https://doi.org/10.1016/j.crte.2012.10.014

DePaolo, D. J., Maher, K., Christensen, J. N., et al., 2006. Sediment Transport Time Measured with U-Series Isotopes: Results from ODP North Atlantic Drift Site 984. *Earth and Planetary Science Letters*, 248 (1/2): 394−410. https://doi.org/10.1016/j.epsl.2006.06.004

Dosseto, A., 2014. Chemical Weathering (U-Series). In: Rink, J. W., Thompson, J. W., eds., Encyclopedia of Scientific Dating Methods. Springer Netherlands, Dordrecht. 152−169. https://doi.org/10.1007/978-94-007-6326-5_246-1

Dosseto, A., Bourdon, B., Gaillardet, J., et al., 2006a. Time Scale and Conditions of Weathering under Tropical Climate: Study of the Amazon Basin with U-Series. *Geochimica et Cosmochimica Acta*, 70 (1): 71−89. https://doi.org/10.1016/j.gca.2005.06.033

Dosseto, A., Bourdon, B., Gaillardet, J., et al., 2006b. Weathering and Transport of Sediments in the Bolivian Andes: Time Constraints from Uranium-Series Isotopes. *Earth and Planetary Science Letters*, 248(3/4): 759−771. https://doi.org/10.1016/j.epsl.2006.06.027

Dosseto, A., Turner, S. P., Douglas, G. B., 2006c. Uranium-Series Isotopes in Colloids and Suspended Sediments: Timescale for Sediment Production and Transport in the Murray-Darling River System. *Earth and Planetary Science Letters*, 246(3/4): 418−431. https://doi.org/10.1016/j.epsl.2006.04.019

Dosseto, A., Bourdon, B., Turner, S. P., 2008. Uranium-Series Isotopes in River Materials: Insights into the Timescales of Erosion and Sediment Transport. *Earth and Planetary Science Letters*, 265(1/2): 1−17. https://

doi.org/10.1016/j.epsl.2007.10.023

Dosseto, A., Buss, H. L., Chabaux, F., 2014. Age and Weathering Rate of Sediments in Small Catchments: The Role of Hillslope Erosion. *Geochimica et Cosmochimica Acta*, 132: 238−258. https://doi. org/10.1016/j.gca.2014.02.010

Dosseto, A., Menozzi, D., Kinsley, L. P. J., 2019. Age and Rate of Weathering Determined Using Uranium-Series Isotopes: Testing Various Approaches. *Geochimica et Cosmochimica Acta*, 246: 213−233. https://doi.org/10.1016/j.gca.2018.11.038

Dunk, R. M., Mills, R. A., Jenkins, W. J., 2002. A Reevaluation of the Oceanic Uranium Budget for the Holocene. *Chemical Geology*, 190(1/2/3/4): 45−67. https://doi.org/10.1016/s0009-2541(02)00110-9

Durand, S., Chabaux, F., Rihs, S., et al., 2005. U Isotope Ratios as Tracers of Groundwater Inputs into Surface Waters: Example of the Upper Rhine Hydrosystem. *Chemical Geology*, 220(1/2): 1−19. https://doi.org/10.1016/j.chemgeo.2005.02.016

Eyal, Y., Olander, D. R., 1990. Leaching of Uranium and Thorium from Monazite: I. Initial Leaching. *Geochimica et Cosmochimica Acta*, 54 (7): 1867−1877. https://doi.org/10.1016/0016-7037(90)90257-L

Fleischer, R. L., 1980. Isotopic Disequilibrium of Uranium: Alpha-Recoil Damage and Preferential Solution Effects. *Science*, 207(4434): 979−981. https://doi.org/10.1126/science.207.4434.979

Fleischer, R. L., 1982. Alpha-Recoil Damage and Solution Effects in Minerals: Uranium Isotopic Disequilibrium and Radon Release. *Geochimica et Cosmochimica Acta*, 46(11): 2191−2201. https://doi.org/10.1016/0016-7037(82)90194-6

Fleischer, R. L., Raabe, O. G., 1978. Recoiling Alpha-Emitting Nuclei. Mechanisms for Uranium-Series Disequilibrium. *Geochimica et Cosmochimica Acta*, 42(7): 973−978. https://doi. org/10.1016/0016-7037(78)90286-7

Fleming, A., Summerfield, M. A., Stone, J. O., et al., 1999. Denudation Rates for the Southern Drakensberg Escarpment, SE Africa, Derived from *in-situ*-Produced Cosmogenic [36]Cl: Initial Results. *Journal of the Geological Society*, 156(2): 209−212. https://doi. org/10.1144/gsjgs.156.2.0209

Granet, M., Chabaux, F., Stille, P., et al., 2010. U-Series Disequilibria in Suspended River Sediments and Implication for Sediment Transfer Time in Alluvial Plains: The Case of the Himalayan Rivers. *Geochimica et Cosmochimica Acta*, 74(10): 2851−2865. https://doi.org/10.1016/j.gca.2010.02.016

Handley, H. K., Turner, S., Afonso, J. C., et al., 2013. Sediment Residence Times Constrained by Uranium-Series Isotopes: A Critical Appraisal of the Comminution Approach. *Geochimica et Cosmochimica Acta*, 103: 245−262. https://doi.org/10.1016/j.gca.2012.10.047

He, L., Tang, Y., 2008. Soil Development along Primary Succession Sequences on Moraines of Hailuogou Glacier, Gongga Mountain, Sichuan, China. *Catena*, 72(2): 259−269. https://doi. org/10.1016/j.catena.2007.05.010

Huckle, D., Ma, L., McIntosh, J., et al., 2016. U-Series Isotopic Signatures of Soils and Headwater Streams in a Semi-Arid Complex Volcanic Terrain. *Chemical Geology*, 445: 68−83. https://doi. org/10.1016/j.chemgeo.2016.04.003

Hussain, N., Lal, D., 1986. Preferential Solution of [234]U from Recoil Tracks and [234]U/[238]U Radioactive Disequilibrium in Natural Waters. *Proceedings of the Indian Academy of Sciences*: *Earth and Planetary Sciences*, 95(2): 245. https://doi.org/10.1007/bf02871869

Keech, A. R., West, A. J., Pett-Ridge, J. C., et al., 2013. Evaluating U-Series Tools for Weathering Rate and Duration on a Soil Sequence of Known

Ages. *Earth and Planetary Science Letters*, 374: 24−35. https://doi.org/10.1016/j.epsl.2013.04.032

Kigoshi, K., 1971. Alpha-Recoil Thorium-234: Dissolution into Water and the Uranium-234/Uranium-238 Disequilibrium in Nature. *Science*, 173 (3991): 47−48. https://doi.org/10.1126/science.173.3991.47

Lasaga, A. C., Blum, A. E., 1986. Surface Chemistry, Etch Pits and Mineral-Water Reactions. *Geochimica et Cosmochimica Acta*, 50(10): 2363−2379. https://doi.org/10.1016/0016-7037(86)90088-8

Lee, V. E., DePaolo, D. J., Christensen, J. N., 2010. Uranium-Series Comminution Ages of Continental Sediments: Case Study of a Pleistocene Alluvial Fan. *Earth and Planetary Science Letters*, 296(3/4): 244−254. https://doi.org/10.1016/j.epsl.2010.05.005

Li, C., Yang, S. Y., Lian, E. G., et al., 2015. A Review of Comminution Age Method and Its Potential Application in the East China Sea to Constrain the Time Scale of Sediment Source-to-Sink Process. *Journal of Ocean University of China*, 14(3): 399−406. https://doi.org/10.1007/s11802-015-2769-8

Li, C., Yang, S. Y., Zhao, J. X., et al., 2016. The Time Scale of River Sediment Source-to-Sink Processes in East Asia. *Chemical Geology*, 446: 138−146. https://doi.org/10.1016/j.chemgeo.2016.06.012

Li, L. F., Chen, J., Chen, T. Y., et al., 2018. Weathering Dynamics Reflected by the Response of Riverine Uranium Isotope Disequilibrium to Changes in Denudation Rate. *Earth and Planetary Science Letters*, 500: 136−144. https://doi.org/10.1016/j.epsl.2018.08.008

Li, L., Chen, J., Chen, Y., et al., 2018. Uranium Isotopic Constraints on the Provenance of Dust on the Chinese Loess Plateau. *Geology*, 46(9): 747−750. https://doi.org/10.1130/g45130.1

Li, L., Chen, J., Hedding, D. W., et al., 2020. Uranium Isotopic Constraints on the Nature of the Prehistoric Flood at the Lajia Site, China. *Geology*, 48(1): 15−18. https://doi.org/10.1130/g46306.1

Li, L., Liu, X. J., Li, T., et al., 2017. Uranium Comminution Age Tested by the Eolian Deposits on the Chinese Loess Plateau. *Earth and Planetary Science Letters*, 467: 64−71. https://doi.org/10.1016/j.epsl.2017.03.014

Li, Z. X., He, Y. Q., Yang, X. M., et al., 2010. Changes of the Hailuogou Glacier, Mt. Gongga, China, Against the Background of Climate Change during the Holocene. *Quaternary International*, 218(1/2): 166−175. https://doi.org/10.1016/j.quaint.2008.09.005

Liang, Z. W., Tian, S. H., 2021. Uranium "Stable" Isotope Fractionation and Its Applications in Earth Science. *Earth Science*, 46(12): 4405−4426. https://doi.org/10.3799/dqkx.2021.091

Lidman, F., Peralta-Tapia, A., Vesterlund, A., et al., 2016. [234]U/[238]U in a Boreal Stream Network—Relationship to Hydrological Events, Groundwater and Scale. *Chemical Geology*, 420: 240−250. https://doi.org/10.1016/j.chemgeo.2015.11.014

Liu, Q., Liu, S. Y., 2009. Seasonal Evolution of Englacial and Subglacial Drainage System of Temperate Glacier Revealed by Hydrological Analysis. *Journal of Glaciology and Geocryology*, 31(5): 857−865 (in Chinese with English Abstract)

Liu, Q., Liu, S. Y., Zhang, Y., et al., 2010. Recent Shrinkage and Hydrological Response of Hailuogou Glacier, a Monsoon Temperate Glacier on the East Slope of Mount Gongga, China. *Journal of Glaciology*, 56(196): 215−224. https://doi.org/10.3189/002214310791968520

Lü, X., Versteegh, G. J. M., Song, J. M., et al., 2016. Geochemistry of Middle Holocene Sediments from South Yellow Sea: Implications to Provenance and Climate Change. *Journal of Earth Science*, 27(5): 751−762. https://doi.org/10.1007/s12583-015-0577-0

Ma, L., Chabaux, F., Pelt, E., et al., 2012. The Effect of Curvature on Weathering Rind Formation: Evidence from Uranium-Series Isotopes in Basaltic Andesite Weathering Clasts in Guadeloupe. *Geochimica et Cosmochimica Acta*, 80: 92−107. https://doi.org/10.1016/j.gca.2011.11.038

Ma, L., Dosseto, A., Gaillardet, J., et al., 2019. Quantifying Weathering Rind Formation Rates Using in Situ Measurements of U-Series Isotopes with Laser Ablation and Inductively Coupled Plasma-Mass Spectrometry. *Geochimica et Cosmochimica Acta*, 247: 1−26. https://doi.org/10.1016/j.gca.2018.12.020

Maher, K., DePaolo, D. J., Christensen, J. N., 2006. U-Sr Isotopic Speedometer: Fluid Flow and Chemical Weathering Rates in Aquifers. *Geochimica et Cosmochimica Acta*, 70(17): 4417−4435. https://doi.org/10.1016/j.gca.2006.06.1559

Maher, K., DePaolo, D. J., Lin, J. C. F., 2004. Rates of Silicate Dissolution in Deep-Sea Sediment: In Situ Measurement Using [234]U/[238]U of Pore Fluids. *Geochimica et Cosmochimica Acta*, 68(22): 4629−4648. https://doi.org/10.1016/j.gca.2004.04.024

Moreira-Nordemann, L. M., 1980. Use of [234]U/[238]U Disequilibrium in Measuring Chemical Weathering Rate of Rocks. *Geochimica et Cosmochimica Acta*, 44(1): 103−108. https://doi.org/10.1016/0016-7037(80)90180-5

Nagy, K. L., Lasaga, A. C., 1992. Dissolution and Precipitation Kinetics of Gibbsite at 80 ºC and pH3: The Dependence on Solution Saturation State. *Geochimica et Cosmochimica Acta*, 56(8): 3093−3111. https://doi.org/10.1016/0016-7037(92)90291-p

Nasdala, L., Wenzel, M., Vavra, G., et al., 2001. Metamictisation of Natural Zircon: Accumulation Versus Thermal Annealing of Radioactivity-Induced Damage. *Contributions to Mineralogy and Petrology*, 141(2): 125−144. https://doi.org/10.1007/s004100000235

Nesbitt, H. W., Young, G. M., 1982. Early Proterozoic Climates and Plate Motions Inferred from Major Element Chemistry of Lutites. *Nature*, 299(5885): 715−717. https://doi.org/10.1038/299715a0

Owen, L. A., Finkel, R. C., Barnard, P. L., et al., 2005. Climatic and Topographic Controls on the Style and Timing of Late Quaternary Glaciation Throughout Tibet and the Himalaya Defined by [10]Be Cosmogenic Radionuclide Surface Exposure Dating. *Quaternary Science Reviews*, 24(12/13): 1391−1411. https://doi.org/10.1016/j.quascirev.2004.10.014

Parruzot, B., Jollivet, P., Rébiscoul, D., et al., 2015. Long-Term Alteration of Basaltic Glass: Mechanisms and Rates. *Geochimica et Cosmochimica Acta*, 154: 28−48. https://doi.org/10.1016/j.gca.2014.12.011

Pelt, E., Chabaux, F., Innocent, C., et al., 2008. Uranium-Thorium Chronometry of Weathering Rinds: Rock Alteration Rate and Paleo-Isotopic Record of Weathering Fluids. *Earth and Planetary Science Letters*, 276(1/2): 98−105. https://doi.org/10.1016/j.epsl.2008.09.010

Pogge von Strandmann, P. A. E., Burton, K. W., James, R. H., et al., 2010. Assessing the Role of Climate on Uranium and Lithium Isotope Behaviour in Rivers Draining a Basaltic Terrain. *Chemical Geology*, 270(1/4): 227−239. https://doi.org/10.1016/j.chemgeo.2009.12.002

Riebe, C. S., Hahm, W. J., Brantley, S. L., 2017. Controls on Deep Critical Zone Architecture: A Historical Review and Four Testable Hypotheses. *Earth Surface Processes and Landforms*, 42(1): 128−156. https://doi.org/10.1002/esp.4052

Riebe, C. S., Kirchner, J. W., Granger, D. E., et al., 2001. Strong Tectonic and Weak Climatic Control of Long-Term Chemical Weathering Rates. *Geology*, 29(6): 511. https://doi.org/10.1130/0091-7613(2001)0290511: stawcc> 2.0.co;2

Rihs, S., Gontier, A., Voinot, A., et al., 2020. Field Biotite Weathering Rate Determination Using U-Series Disequilibria. *Geochimica et Cosmochimica Acta*, 276: 404−420. https://doi. org/10.1016/j. gca.2020.01.023

Riotte, J., Chabaux, F., 1999. (^{234}U/^{238}U) Activity Ratios in Freshwaters as Tracers of Hydrological Processes: The Strengbach Watershed (Vosges, France). *Geochimica et Cosmochimica Acta*, 63(9): 1263−1275. https://doi.org/10.1016/S0016-7037(99)00009-5

Robinson, L. F., Adkins, J. F., Fernandez, D. P., et al., 2006. Primary U Distribution in Scleractinian Corals and Its Implications for U Series Dating. *Geochemistry*, *Geophysics*, *Geosystems*, 7(5). https://doi. org/ 10.1029/2005gc001138

Robinson, L. F., Henderson, G. M., Hall, L., et al., 2004. Climatic Control of Riverine and Seawater Uranium-Isotope Ratios. *Science*, 305(5685): 851−854. https://doi.org/10.1126/science.1099673

Ruiz-Agudo, E., Putnis, C. V., Rodriguez-Navarro, C., et al., 2012. Mechanism of Leached Layer Formation during Chemical Weathering of Silicate Minerals. *Geology*, 40(10): 947−950. https://doi. org/ 10.1130/g33339.1

Smalley, I., 1995. Making the Material: The Formation of Silt Sized Primary Mineral Particles for Loess Deposits. *Quaternary Science Reviews*, 14(7/8): 645−651. https://doi. org/10.1016/0277-3791(95) 00046-1

Su, H., Dong, M., Hu, Z. B., 2019. Late Miocene Birth of the Middle Jinsha River Revealed by the Fluvial Incision Rate. *Global and Planetary Change*, 183: 103002. https://doi.org/10.1016/j.gloplacha.2019.103002

Su, Z., Song, G. P., Cao, Z. T., 1996. Maritime Characteristics of Hailuogou Glacier in the Gongga Mountains. *Journal of Glaciology and Geocryology*, 18(S1): 51−59 (in Chinese with English Abstract)

Sun, J. M., 2002. Provenance of Loess Material and Formation of Loess Deposits on the Chinese Loess Plateau. *Earth and Planetary Science Letters*, 203(3-4): 845−859. https://doi. org/10.1016/S0012-821x(02) 00921-4

Taylor, A., Blum, J. D., 1995. Relation between Soil Age and Silicate Weathering Rates Determined from the Chemical Evolution of a Glacial Chronosequence. *Geology*, 23(11): 979−982. https://doi. org/ 10.1130/0091-7613(1995)0230979: rbsaas> 2.3.co;2

Thollon, M., Bayon, G., Toucanne, S., et al., 2020. The Distribution of (^{234}U/^{238}U) Activity Ratios in River Sediments. *Geochimica et Cosmochimica Acta*, 290: 216−234. https://doi. org/10.1016/j. gca.2020.09.007

Vigier, N., Bourdon, B., Turner, S., et al., 2001. Erosion Timescales Derived from U-Decay Series Measurements in Rivers. *Earth and Planetary*

Science Letters, 193(3/4): 549−563. https://doi. org/10.1016/S0012-821x(01)00510-6

Wang, J., Pan, B. T., Zhang, G. L., et al., 2013. Late Quaternary Glacial Chronology on the Eastern Slope of Gongga Mountain, Eastern Tibetan Plateau, China. *Science China Earth Sciences*, 56(3): 354−365. https://doi.org/10.1007/s11430-012-4514-0

Wang, R. M., You, C. F., 2013a. Uranium and Strontium Isotopic Evidence for Strong Submarine Groundwater Discharge in an Estuary of a Mountainous Island: A Case Study in the Gaoping River Estuary, Southwestern Taiwan. *Marine Chemistry*, 157: 106−116. https://doi. org/10.1016/j.marchem.2013.09.004

Wang, R. M., You, C. F., 2013b. Precise Determination of U Isotopic Compositions in Low Concentration Carbonate Samples by MC-ICP-MS. *Talanta*, 107: 67−73. https://doi.org/10.1016/j.talanta.2012.12.044

White, A. F., Blum, A. E., Schulz, M. S., et al., 1996. Chemical Weathering Rates of a Soil Chronosequence on Granitic Alluvium: I. Quantification of Mineralogical and Surface Area Changes and Calculation of Primary Silicate Reaction Rates. *Geochimica et Cosmochimica Acta*, 60(14): 2533−2550. https://doi.org/10.1016/0016-7037(96)00106-8

White, A. F., Brantley, S. L., 2003. The Effect of Time on the Weathering of Silicate Minerals: Why do Weathering Rates Differ in the Laboratory and Field?. *Chemical Geology*, 202(3/4): 479−506. https://doi. org/ 10.1016/j.chemgeo.2003.03.001

White, A. F., Schulz, M. S., Stonestrom, D. A., et al., 2009. Chemical Weathering of a Marine Terrace Chronosequence, Santa Cruz, California. Part II: Solute Profiles, Gradients and the Comparisons of Contemporary and Long-Term Weathering Rates. *Geochimica et Cosmochimica Acta*, 73(10): 2769−2803. https://doi. org/10.1016/j. gca.2009.01.029

White, A. F., Schulz, M. S., Vivit, D. V., et al., 2008. Chemical Weathering of a Marine Terrace Chronosequence, Santa Cruz, California I: Interpreting Rates and Controls Based on Soil Concentration-Depth Profiles. *Geochimica et Cosmochimica Acta*, 72(1): 36−68. https://doi. org/10.1016/j.gca.2007.08.029

Zhou, J., Bing, H. J., Wu, Y. H., et al., 2016. Rapid Weathering Processes of a 120-Year-Old Chronosequence in the Hailuogou Glacier Foreland, Mt. Gongga, SW China. *Geoderma*, 267: 78−91. https://doi. org/ 10.1016/j.geoderma.2015.12.024

Zielinski, R. A., Peterman, Z. E., Stuckless, J. S., et al., 1982. The Chemical and Isotopic Record of Rock-Water Interaction in the Sherman Granite, Wyoming and Colorado. *Contributions to Mineralogy and Petrology*, 78(3): 209−219. https://doi.org/10.1007/bf00398915